

## A Toeplitz representation for repulsive systems

This article has been downloaded from IOPscience. Please scroll down to see the full text article.

1983 J. Phys. A: Math. Gen. 16 L19

(<http://iopscience.iop.org/0305-4470/16/1/005>)

View [the table of contents for this issue](#), or go to the [journal homepage](#) for more

Download details:

IP Address: 129.252.86.83

The article was downloaded on 30/05/2010 at 16:11

Please note that [terms and conditions apply](#).

## LETTER TO THE EDITOR

# A Toeplitz representation for repulsive systems

Asher Baram

Department of Chemical Physics, Weizmann Institute of Science, Rehovot 76100, Israel

Received 13 September 1982

**Abstract.** A new method is presented for the calculation of thermodynamic properties of ensembles of particles interacting via repulsive forces. A tridiagonal matrix representation is constructed in terms of the cluster integrals. Its asymptotic form is utilised to obtain very good numerical estimates of the thermodynamic properties. Moreover, it is shown that the fluid branch may terminate at a critical activity  $z_c$ , which is identical to the activity at the fluid-solid transition. A relation is found between  $z_c$  and the radius of convergence of the activity series via the asymptotic matrix elements.

Much evidence points to the fact that the structure of a liquid is determined primarily by the short-range repulsive forces. The longer-range attractive part of the potential is relatively weak and, as far as the structure is concerned, can be treated as a perturbation (Barker and Henderson 1976). A variety of continuum fluid models, and less realistic but mathematically simpler lattice models, are available for studying the effects of the repulsive forces on the equations of state and in particular on the properties of the fluid-solid melting transition. All the information about the fluid phase is contained in the well known Mayer expansion of the grand partition function in powers of the activity  $z$ . The pressure is given by the standard relation

$$\beta p = \sum_{l=1}^{\infty} b_l z^l \quad (1)$$

where  $\beta = 1/kT$  and the  $b_l$  are the well known cluster integrals (cluster sums for lattice models) with  $b_1 = 1$ . The number density follows from (1) as

$$\rho = z \frac{d}{dz} (\beta p) = \sum_{l=1}^{\infty} l b_l z^{l-1}. \quad (2)$$

For all repulsive potentials the coefficients  $b_l$  alternate regularly in sign and increase rapidly in magnitude (Groeneveld 1962). This indicates the existence of a non-physical singularity on the negative  $z$  axis close to the origin. The physically relevant region is far outside the radii of convergence of the low-density series, and it is usually fitted using Padé approximants (Gaunt and Fisher 1965, Baxter *et al* 1980) or Levin approximants (Baram and Luban 1979, 1982). In all cases the series are represented in terms of a large number of poles on the negative  $z$  axis, suggesting a branch cut on part of the negative  $z$  axis. However, none of the approximants exhibit physically relevant poles on or near the positive real  $z$  axis.

In this letter we use a matrix representation whose elements are determined by the cluster integrals to obtain simple expressions which are good numerical estimates

of the thermodynamic properties of the fluid branch. These expressions exhibit, in the majority of the cases, square-root-like singularities on the positive real  $z$  axis, which define the domain of existence of the fluid phase. Consider the symmetric tridiagonal matrix  $R$  defined by the requirement

$$(R^{n-1})_{11} = |b_n|. \quad (3)$$

Then the pressure is given by

$$\beta p(z) = [\mathbf{1}(1/z) + R]_{11}^{-1} \quad (4)$$

where  $\mathbf{1}$  is the infinite unit matrix. Similarly  $\bar{R}$  is defined by the relation

$$(\bar{R}^{n-1})_{11} = n|b_n| \quad (5)$$

and the density is given by

$$\rho(z) = [\mathbf{1}(1/z) + \bar{R}]_{11}^{-1}. \quad (6)$$

It has been shown by Gordon (1968) that for non-decreasing functions of  $z$  the matrix elements of the corresponding matrices are non-negative. As a result a sequence of even and odd truncations of the matrices provides a sequence of successively improving lower and upper bounds respectively for these functions. The  $n$ th even truncation is obtained by setting  $R_{n,n+1} = R_{n+1,n} = 0$  and then inverting the resulting finite  $n \times n$  matrix, based on the first  $2n$  cluster integrals. The  $n$ th odd truncation corresponds to the solution of the same  $n \times n$  matrix but with  $R_{nn}$  replaced by the finite continued fraction

$$R_{n-1,n-1} = \frac{R_{n-1,n}^2}{R_{n-2,n-1} + \frac{R_{n-2,n}^2}{R_{n-3,n-2} + \frac{R_{n-3,n-2}^2}{R_{n-3,n-3} + \dots}}.$$

Here the matrix elements depend on the first  $(2n-1)$  cluster integrals. The first few approximants may be easily derived to give

$$\frac{z}{1 + |b_2|z} < \beta p(z) < z \quad (6a)$$

$$\frac{z(1 + R_{22}z)}{1 + (|b_2| + R_{22})z + (|b_2|R_{22} - b_3 + b_2^2)z^2} < \beta p(z) < \frac{z[|b_2| + (b_3 - b_2^2)z]}{|b_2| + b_3z} \quad (6b)$$

where

$$R_{22} = \frac{|b_4| - b_3|b_2|}{b_3 - b_2^2} - |b_2|.$$

Similar expressions may be derived for  $\rho(z)$ . At the low-density limit the approximants converge smoothly and rapidly as  $n$  increases. However, for finite  $n$  and large enough  $z$  the lower bound converges to a constant, while the upper bound is of the form  $z/c_1$  where  $c_1$  is a constant. Better approximations for the high-activity regime require some knowledge about the asymptotic properties of the representation matrices. It seems that for repulsive systems the matrix elements converge to constants along the diagonals (see tables 1 and 2). Using this property we partition each of the infinite matrices into two submatrices. A finite  $n_0 \times n_0$  submatrix is coupled to an infinite

**Table 1.** Matrix elements of  $R$  for various models. Uncertainties in last digits of  $B$  and  $A$  for the simple cubic model, due to uncertainties in  $z_c$ , are shown in parentheses.

	Model†						
	HSL	HHL	SCL	HL $d = 1$	PHS	Gaussian $d = 1$	Gaussian $d = 3$
$R_{11}$	2.5	3.5	3.5	1.0	2.0	1.0	1.0
$R_{12}$	2.0207	2.6615	3.0139	0.7071	1.5811	0.7842	0.9336
$R_{22}$	3.9694	5.2647	6.1972	1.3333	3.1556	1.4916	2.0401
$R_{23}$	2.0715	2.7426	3.2666	0.6872	1.6392	0.7639	1.0681
$R_{33}$	4.1008	5.4274	6.4619	1.3490	3.2539	1.5058	2.1527
$R_{34}$	2.0861	2.7596	3.3299	0.6832	1.6508	0.7604	1.0932
$R_{44}$	4.1340	5.4789	6.5364	1.3537			
$R_{45}$	2.0942	2.7660	3.3639	0.6817			
$R_{55}$	4.1453	5.5018	6.5446	1.3557			
$R_{56}$	2.0994	2.7691	3.3963	0.6810			
$R_{66}$	4.1485	5.5138		1.3568			
$R_{67}$	2.104	2.7708		0.6806			
$R_{77}$	4.1468	5.5208		1.3574			
$R_{78}$	2.1087	2.7720		0.6803			
$R_{88}$		5.5251		1.3578			
$R_{89}$		2.7729		0.6801			
$R_{99}$		5.5279		1.3581			
Exact asymptotic values							
$R_{nn}$	4.0559	5.50	6.26 (3)	$\frac{1}{2}e = 1.3591$			
$R_{n,n+1}$	2.1597	2.7951	3.60 (1)	$\frac{1}{4}e = 0.6796$			

† HSL, hard-square lattice; HHL, hard-hexagon lattice; SCL, simple cubic lattice; HL, hard lines; PHS, parallel hard squares.

tridiagonal Toeplitz matrix with  $B$  and  $A$  as constant diagonal and off-diagonal elements respectively. (A discussion of Toeplitz matrices and determinants is given by Grenander and Szegö (1958).) The upper submatrix contains the exact contribution of a group of  $2n_0$  particles to the thermodynamic functions. The infinite Toeplitz tail approximates the contribution of the infinite system to the macroscopic observables. The infinite tail can be handled easily and its net effect is to add to  $R_{n_0n_0}$  (the last element of the exact submatrix) the correction term  $Ag(z)$ , where

$$g(z) = -\frac{B+z^{-1}}{2A} + \left[ \left( \frac{B+z^{-1}}{2A} \right)^2 - 1 \right]^{1/2} \tag{7}$$

is the positive root of the characteristic quadratic equation

$$Ag^2(z) + (B+z^{-1})g(z) + A = 0. \tag{8}$$

At the low-density limit  $g(z)$  vanishes like  $z$ , and the contribution of the infinite tail is negligible. The macroscopic observables are completely determined at this limit by a finite group of particles. For higher activity values the correction term becomes significant, and the properties of the system depend on the uniform tail. For the case  $B < 2A$  the square root term in  $g(z)$  vanishes for  $z_c$  fulfilling the equation

$$1/z_c = 2A - B. \tag{9}$$

For  $z > z_c$   $g(z)$  and the resulting thermodynamic functions become complex. Thus

Table 2. As in table 1 but for elements of  $\bar{R}$ .

	Model <sup>†</sup>						Gaussian $d = 3$
	HSL	HHL	SCL	HL $d = 1$	PHS	Gaussian $d = 1$	
$R_{11}$	5.0	7.0	7.0	2.0	4.0	2.0	2.0
$R_{12}$	2.4495	3.0	3.8730	0.7071	1.8708	0.9194	1.2709
$R_{22}$	4.0	5.5556	6.5333	1.3333	3.3016	1.4310	2.2453
$R_{23}$	2.1985	2.8523	3.5377	0.6872	1.7102	0.7715	1.1487
$R_{33}$	4.1379	5.5067	6.4873	1.3490	3.3151	1.4999	2.2322
$R_{34}$	2.1438	2.8280	3.5304	0.6832	1.6825	0.7620	1.1292
$R_{44}$	4.1237	5.4917	6.4167	1.3537			
$R_{45}$	2.1522	2.8187	3.5462	0.6817			
$R_{55}$	4.0881	5.4877	6.3483	1.3557			
$R_{56}$	2.1591	2.8124	3.5701	0.6810			
$R_{66}$	4.0749	5.4889		1.3568			
$R_{67}$	2.1596	2.8079		0.6806			
$R_{77}$	4.0742	5.4929		1.3574			
$R_{78}$	2.1545	2.8035		0.6803			
$R_{88}$		5.4979		1.3578			
$R_{89}$		2.7995		0.6801			
$R_{99}$		5.5029		1.3581			
Exact asymptotic values							
$R_{nn}$	4.0559	5.5	6.26 (3)	$\frac{1}{2}e = 1.3591$			
$R_{n,n+1}$	2.1597	2.7951	3.60 (1)	$\frac{1}{4}e = 0.6796$			

<sup>†</sup> HSL, hard square on lattice; HHL, hard hexagons on lattice; SCL, simple cubic lattice; HL, hard lines; PHS, parallel hard squares.

the fluid phase terminates at  $z_c$ . For the case  $B \geq 2A$  the grand partition function and its logarithm are analytic for all  $z > 0$ , and the fluid regime exists in the entire physical region. On the negative real  $z$  axis the square root term always vanishes at  $-z_0$  defined by the equality

$$1/z_0 = 2A + B. \quad (10)$$

Obviously  $z_0 < z_c$  and therefore this non-physical singularity determines the radii of convergence of the series, and the asymptotic form of the cluster integrals

$$|b_{n+1}/b_n| = (2A + B)(1 + O(n^{-1})). \quad (11)$$

The functions are complex in the region  $-\infty < z < -z_0$  provided  $2A > B$ , or in the region  $(2A - B)^{-1} < z < -z_0$  for  $B > 2A$ . This complex domain, common to all repulsive systems, is analogous to the branch cut found to extend along the negative real axis from  $-z_0$ , for one-dimensional hard lines and the repulsive van der Waals gas (Hiis Hauge and Hemmer 1963). Numerical analysis strongly suggests that such a branch cut is a characteristic feature of repulsive models (Gaunt and Fisher 1965).

It is interesting to compare the results of the Toeplitz representation with those obtained from the few models solved exactly. The continuum one-dimensional hard-lines model obeys the well known equations of state

$$\beta p = \rho/(1 - \rho) \quad \beta p \exp(\beta p) = z \quad (12)$$

where the hard-core diameter  $\sigma = 1$ . The positive real  $z$  axis is free of singularities;

the closest singularity is a square-root-type branch point at  $-z_0 = -1/e$ . Using equations (9) and (10) one obtains  $B = 2A = \frac{1}{2}e = 1.3591$ . These 'exact asymptotic values' exhibit the fast convergence of the matrix elements to their limiting constant values (see tables 1 and 2). In figure 1 the Toeplitz approximation, based on a  $3 \times 3$  finite matrix and the exact asymptotic values, to the number density  $\rho(z)$  is compared with the exact solution of equations (12). Up to  $z = 25$  the two curves are indistinguishable; for higher  $z$  values the approximation still provides very good numerical estimates. Upper and lower bounds based on the same finite matrix provide good numerical estimates up to  $z \sim 6$ .

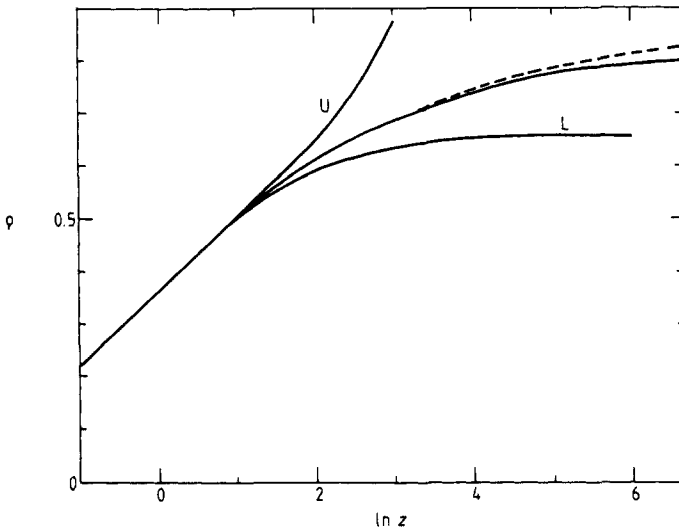


**Figure 1.** One-dimensional hard lines. Plot of the number density against  $\ln z$ . Full curve, Toeplitz approximation based on a  $3 \times 3$  matrix and  $B = 2A = \frac{1}{2}e$ ; broken curve, exact solution; curve U, upper bound based on  $3 \times 3$  matrix; curve L, lower bound based on five coefficients.

The hard-hexagon lattice model has been solved rigorously by Baxter (1980). The model has a critical point corresponding to a fluid–solid transition at  $z_c = \frac{1}{2}(11 + 5\sqrt{5}) = 11.09017$  with a critical exponent  $\alpha = \frac{1}{3}$ . The radius of convergence of the activity series is  $z_0 = 1/z_c = 0.090169$ , due to a  $\frac{5}{2}$ -type singularity located at  $-z_0$ . Employing these values one obtains  $B = \frac{1}{2}(z_c - 1/z_c) = 5.50$   $A = \frac{1}{4}(z_c + 1/z_c) = 2.7951$  in close agreement with the matrix elements of  $\bar{R}$ . Thus the termination point of the fluid branch may be identified with the fluid–solid critical point. The pressure is less sensitive than  $\rho(z)$  to  $z_c$ , since its singular term is masked by the leading linear term in the vicinity of  $z_c$ . Therefore the elements of  $R$  predict values for  $z_c$  which are too high. Nevertheless the numerical estimations to the pressure are highly accurate. In figure 2 an approximation to  $\beta p(z)$ , based on a  $3 \times 3$  exact matrix and a Toeplitz correction with  $A = R_{34}$ ,  $B = R_{44}$ , is shown and compared with the exact solution. Knowledge of the first eight cluster integrals is required in order to construct this approximation. Although the hard-square lattice model has not been solved rigorously the locations of its characteristic singularities are known to high accuracy. Baxter *et al* (1980) obtained the first 24 terms of the high-density series in terms of  $1/z$  for the order parameter, and from

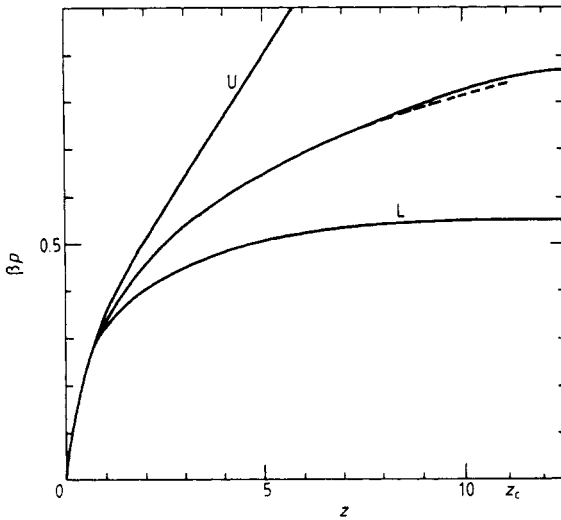


**Figure 2.** Hard-hexagon lattice model: plot of pressure against activity. Full curve, Toeplitz approximation based on  $3 \times 3$  matrix and  $B = R_{44}$ ,  $A = R_{34}$ ; broken curve, exact solution; curve U, upper bound derived using six coefficients; curve L, lower bound derived using five coefficients.

these estimated  $z_c$  to be 3.7962(1). Similarly  $z_0$  is estimated to be 0.1194(1), resulting in  $A = 2.1597$  and  $B = 4.0559$ , again in very good agreement with the elements of  $\bar{R}$ .

The Toeplitz assumption results in universal, dimensionality-independent, critical exponents. More precisely, near the fluid–solid transition (if it exists) the number density is given by

$$\rho(z) = \rho_c - c(z_c - z)^{1/2} \quad (13)$$

while the compressibility diverges as  $(z_c - z)^{-1/2}$ . Near the non-physical singularity at  $-z_0$  the density diverges as  $(z_0 + z)^{-1/2}$ . This classical-like result is wrong; the characteristic critical exponent  $\alpha$  is model dependent at the freezing transition (Baxter 1980). Similarly the divergence of the density at  $z_0$  is model dependent. Thus the exact critical exponents depend on the small deviations from the constant asymptotic values, although their effect on the isotherms and the location of the critical points is negligible.

The particle–hole symmetry may be used to derive high-density expansions in terms of  $1/z$  about closest packing for lattice models. (It is not known how to obtain the analogous expansions for continuum models.) Unfortunately the signs of the coefficients do not behave regularly, and it is impossible to apply the present method. The hard-square lattice is exceptional because the coefficients of its expansions alternate in sign. Thus it is possible to derive the sequence of bounds, which are very effective since the radius of convergence is of the order of  $1/z_c$ . However, the matrix elements do not exhibit any Toeplitz form.

Finally it should be remarked that a very similar asymptotic convergence to constant terms occurs in rotational relaxation processes (Baram 1980). The spectral lineshape function is given by an equation similar to equation (4), where  $R$  is the relaxation matrix and  $1/z$  is the frequency variable. The elements of the relaxation matrix are related to the Clebsch–Gordan coefficients that tend asymptotically to their classical constant limiting values. Thus the relaxation matrix contains a small finite submatrix

corresponding to low rotational states, coupled to an infinite classical Toeplitz tail. At the fast-motion limit (analogous to the low-density limit) the tail is irrelevant, while at the slow-motion limit it determines the characteristic features of the spectral lineshape function.

**References**

- Baram A 1980 *Mol. Phys.* **41** 823–31  
Baram A and Luban M 1979 *J. Phys. C: Solid State Phys.* **12** L659–64  
— 1982 to be published  
Barker J A and Henderson D 1976 *Rev. Mod. Phys.* **48** 587  
Baxter R J 1980 *J. Phys. A: Math. Gen.* **13** L61–70  
Baxter R J, Enting I G and Tsang S K 1980 *J. Stat. Phys.* **22** 465–89  
Gaunt D S and Fisher M E 1965 *J. Chem. Phys.* **43** 2840–63  
Gordon R G 1968 *J. Math. Phys.* **9** 655–63  
Grenander U and Szegö G 1958 *Toeplitz Forms and Their Applications* (Berkeley: UC Press)  
Groeneveld J 1962 *Phys. Lett.* **3** 50–1  
Hiis Hauge E and Hemmer P C 1963 *Physica* **29** 1338–44